Chapter 4

OVERWASH SEDIMENT TRANSPORT:

DETAILED FIELD STUDIES

4.1. INTRODUCTION

Despite the variety of studies related to overwash processes and washover dynamics and evolution, there is still a lack of knowledge of short-term overwash sediment transport and its relation to the oceanographic conditions. The integrated analysis of a data-set including the main morphodynamic quantities (transverse profile change, mixing depth, and sediment transport patterns on beach and washovers), overwash flow velocities, and oceanographic conditions associated with an overwash event has not been found in the literature. Non-storm overwash events have not been widely studied, however they have some advantages for fieldwork data collection: their occurrence is more predictable than the storm-overwash, the deployment of instrumentation on the beach is less hazardous, the magnitude of overwash processes is still preserved, and it is representative of overwash situations in low-lying barriers.

In situ measurements of sediment transport induced by overwash flows are scarce, and no application of tracers was found in the literature. Sediment transport studies using fluorescent tracers have been very important in the development of theories that are nowadays widely used by coastal scientists and engineers (Vila-Concejo *et al.*, 2003b). Studies showed that fluorescent tracers could be used for a variety of purposes like the quantification of sediment transport on swash platforms (Oertel, 1972), and on submarine sand banks (Collins *et al.*., 1995), longshore sediment transport (e.g. Komar and Inman, 1970; Ciavola *et al.*, 1997), harbour infilling processes (Ferreira *et al*., 2002), and tidal inlet margins (Vila-Concejo *et al*., 2004). The determination of the mixing depth is critical to understand the depth to which the flux disturbs the sand (King, 1951), however this measurements has only been done occasionally for overwash flows (Fisher *et al*., 1974; Leatherman, 1976; Leatherman and Zaremba, 1987). Some studies of the hydraulics of overwash flow were found in the literature

using different fieldwork techniques (e.g. Leatherman, 1977; Leatherman and Zaremba, 1987; Holland *et al*., 1991; Bray and Carter, 1992; Guillén *et al*., 1994).

The objective of this work is to characterise the dynamics of non-storm overwash processes and to understand the importance of non-storm overwash *versus* storm-overwash. For that purpose innovative data sets were obtained, including measurements of overwash-induced morphology variations, oceanographic conditions, mixing depth and sediments transport patterns induced by overwash flows in washover plains and lobes.

4.2. METHODS

4.2.1. FIELDWORK DATA COLLECTION

Fieldwork was planned for conditions when non-storm overwash was expected to occur. These conditions result generally from a combination of three factors: winter wave heights, high spring tide, and low elevation frontal areas. Three fieldwork campaigns were performed on the same site and named GO.1 (February 9th and 10th 2001), GO.2 (January 31th and February 1st 2002), and GO.3 (18th and 19th February 2003). All fieldwork campaigns were performed under maritime winter conditions, which were defined to occur on the Portuguese Coast between October and March. For the GO.1, GO.2 and GO.3 campaigns the expected spring high tide elevation was 1.8 m, 1.6 m, and 1.7 m above MSL, respectively. The fieldwork was performed on low-lying portions on the western part of Barreta Island (Figure 4.1): on a washover plain (GO.1 and GO.3), and on washover lobes (GO.2 and GO.3, Figure 4.2). Overwash occurred during two of the fieldwork campaigns (GO.1 and GO.3), and therefore GO.2 will not be extensively detailed in the text. The settings of the GO.1 and GO.3 fieldwork campaigns are on Figures 4.3 and 4.4, respectively.

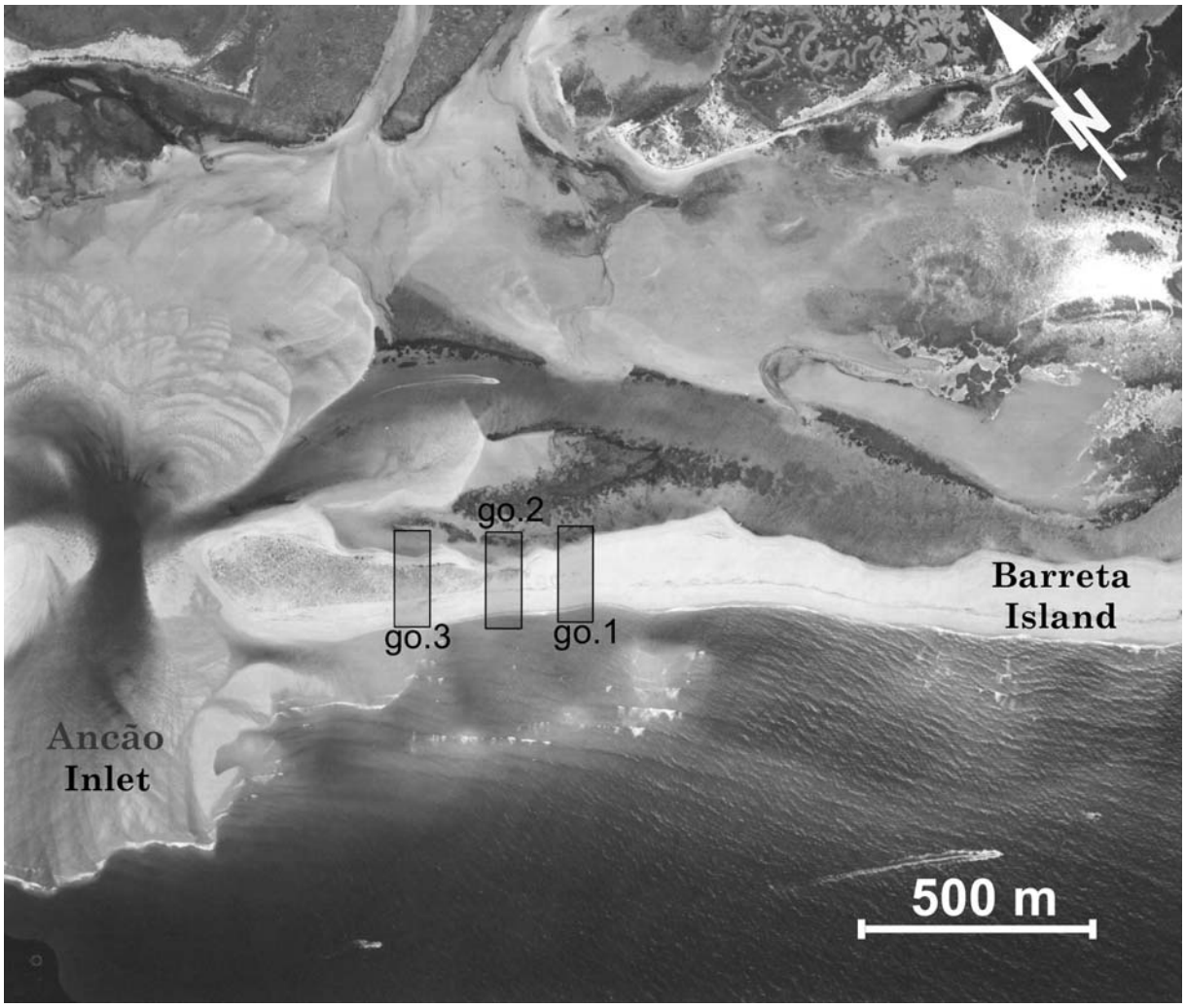

Figure 4.1. Location of fieldwork campaigns GO.1, GO.2 and GO.3 on Barreta Island. The vertical aerial photograph was taken in August 2001.The GO.2 and GO.3 fieldwork campaigns were made on washover lobes which did not exist at the time of this photograph.

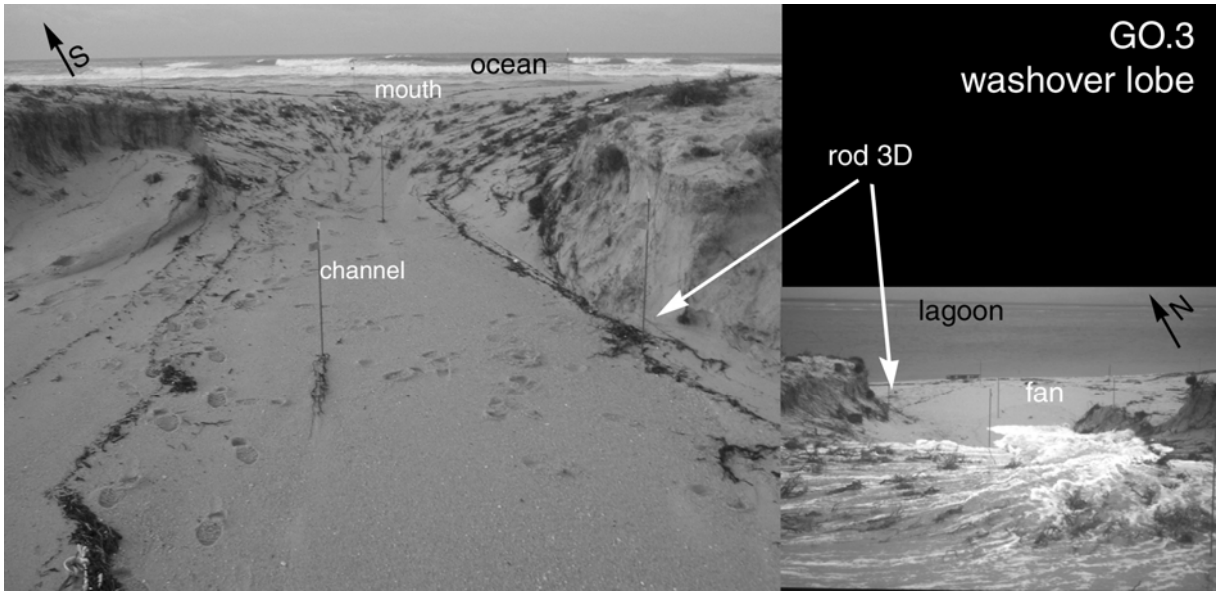

Figure 4.2. Photographs of the GO.3 washover lobe, without and with overwash flow.

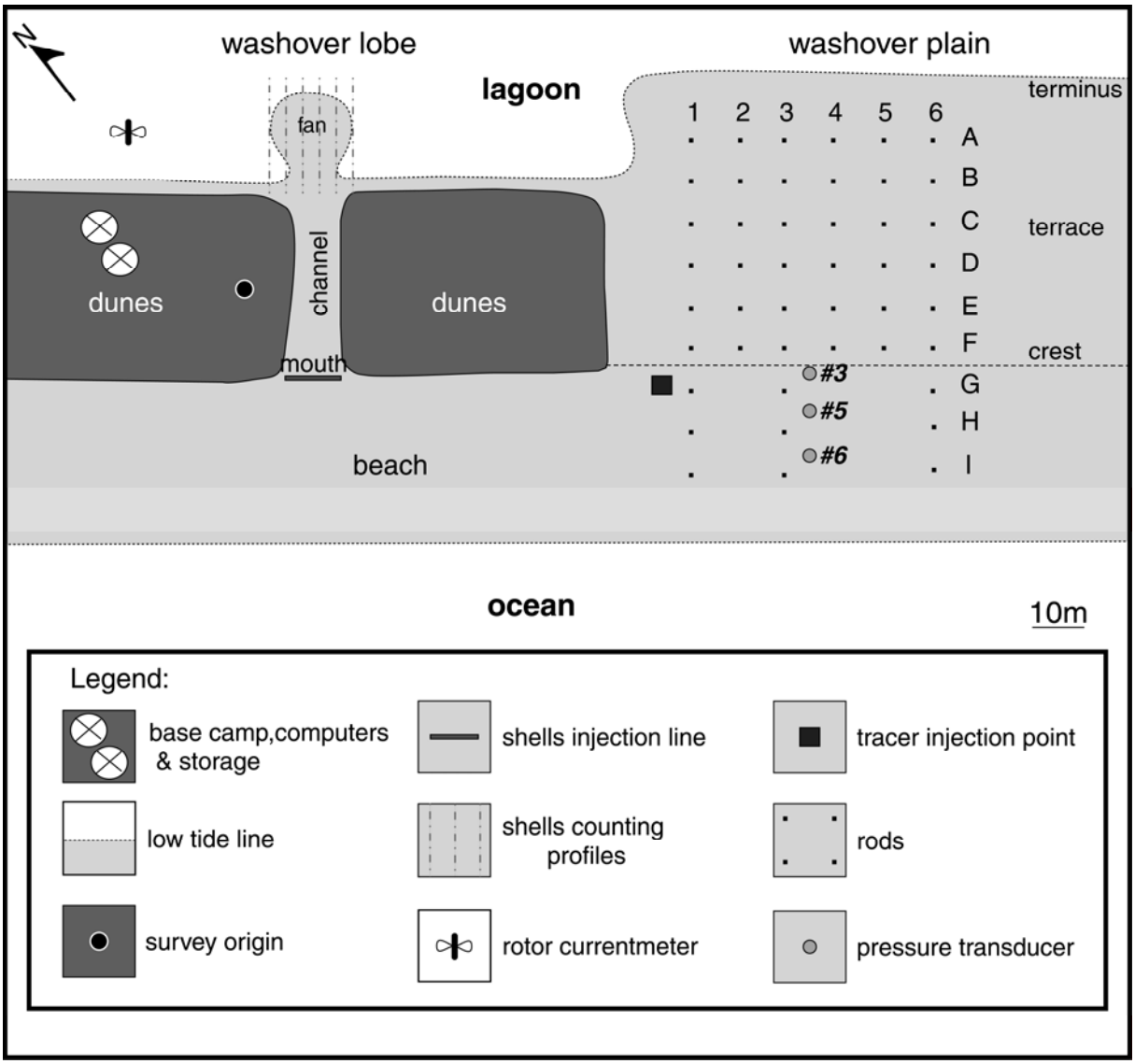

Figure 4.3. Setting of the GO.1 fieldwork campaign.

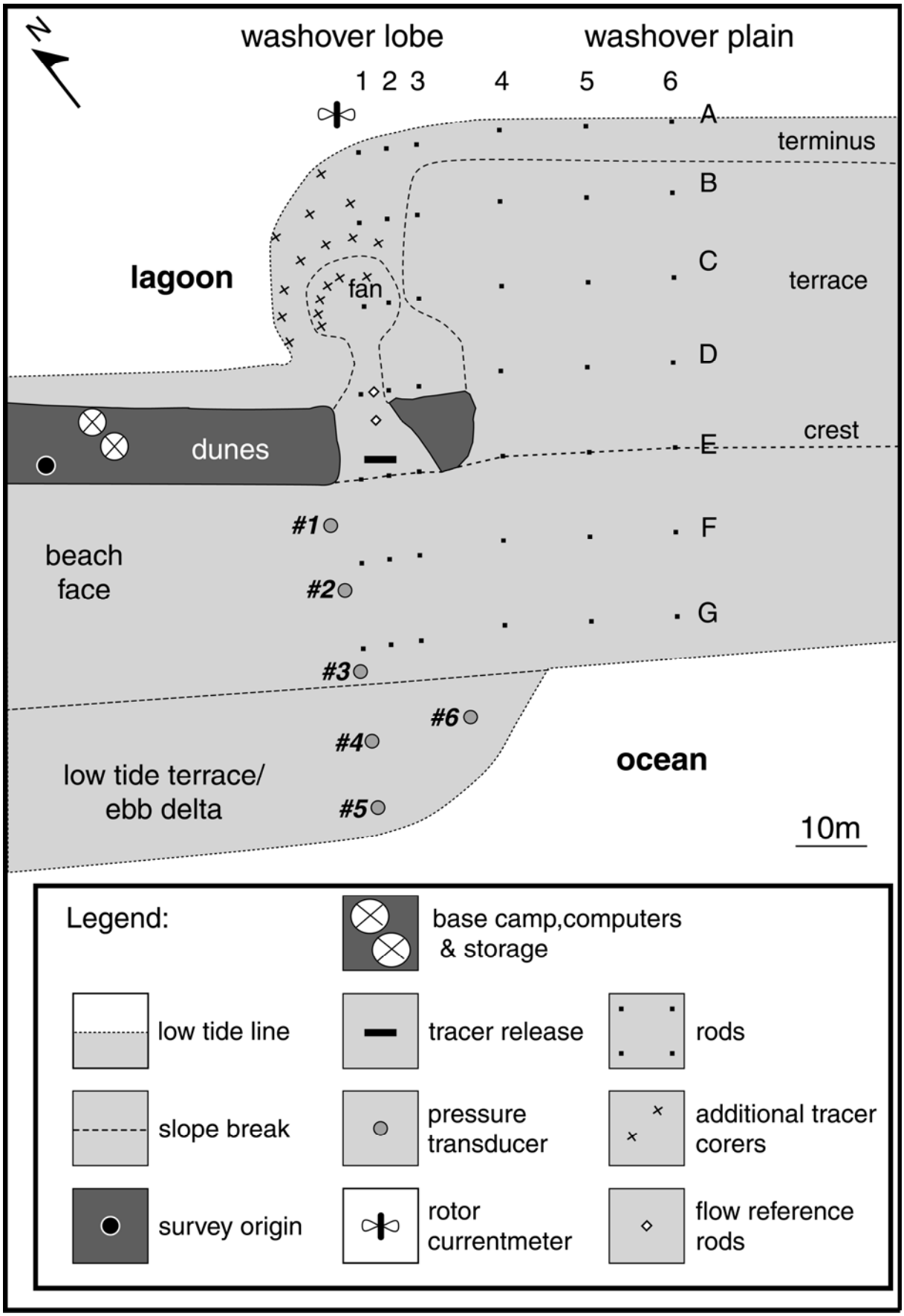

Figure 4.4. Setting of the GO.3 fieldwork campaign.

4.2.1.1. Forcing mechanisms

A set of six pressure transducers (PT) was placed on the beach, at low tide. All PT's had a sample rate of 4 Hz, and were independently connected to a data logger. During GO.1, the PT's were placed across-shore, three on the beach face and three on the seaward and the mid-part of the washover terrace (Figure 4.3). During GO.3, the PTs were placed across-shore from the low tide terrace to the upper beach face (Figure 4.4).

In the lagoon, at the tidal channel margin (Figures 4.3 and 4.4), a self-logging currentmeter was placed, at about 90 cm from the bottom. The equipment incorporated a PT, and the data was collected at a rate of 0.1 Hz, as 1-min bursts.

4.2.1.2. Overwash flow

The overwash occurrences were estimated using the PTs that was located on the top of the beach, closest to the washover crest or washover mouth [PT3 on GO.1 (Figure 4.3) and PT1 on GO.3 (Figure 4.4)]. These PTs recorded the intermittent water depth at the top of the beach face, and therefore provided an estimate of the frequency of overwash flows.

During GO.3 the overwash velocity was measured by timing the passage of the overwash water front between rods located at the washover channel (Figure 4.4). Simultaneously, a flow meter was used at the same location but the presence of the instrument and especially of the operator interfered significantly with the flow. The obtained measurements were considered unreliable, and because of the nature of overwash flow any type of instrumentation deployed in the area would induce too much interference on the flow.

An indirect measurement of maximum overwash flow intrusion was made during GO.1 through the placement of marked shells on a washover lobe, near the studied washover plain (Figure 4.3). The shells were painted with green paint, and placed as a line on the washover mouth. After the overwash event, 13 cross-shore profiles were defined on the washover fan,

3 m apart (Figure 4.3). For every profile, a measuring tape was placed on the fan and the number and position of marked shells was recorded.

4.2.1.3. Topography

For GO.1, a grid of rods was established over the beach, the washover crest, and the washover terrace, until the washover terminus (Figure 4.3). The 10 m×10 m grid was made of 6 cross-shore profiles (1 to 6 in Figure 4.3), and 9 longshore profiles (A to I in Figure 4.3), covering an area of about 4,000 m^2.

For GO.3, two grids of rods were established, one on a washover lobe and another on a washover plain, both covering the adjacent beach (Figure 4.4). An irregular grid was made, consisting of three cross-shore profiles on the washover lobe (1 to 3 in Figure 4.4), 4 m apart, and three cross-shore profiles on the washover plain (4 to 6 in Figure 4.4), 12 m apart. For both areas, 7 longshore profiles were defined (A to G in Figure 4.4), 10 to 12 m apart. To have more detailed data from the washover channel, two sampling points were added (flow reference rods in Figure 4.4) along the channel axis, at 8 m and 12 m from the washover mouth.

Surveys were made using a total station (GO.1) and a real-time kinematic RTK-DGPS, recording at 1 Hz (GO.3). During both fieldwork campaigns surveys were conducted before and after overwash, and the rod heights were measured every 30 minutes, during the overwash event.

4.2.1.4. Mixing depth

The method followed for mixing depth determination was based on the procedures described for beach experiments in Ferreira *et al.* (2000). It was firstly necessary to obtain contrasting sand. For GO.1, the preparation of the sand entailed collecting sediment from the

study area, washing to eliminate salt, and dying with green ink. For GO.3, about 30 kg of heavy mineral sand was collected from a placer deposit at a beach, 14 km to the west of the study area. The measurements of mixing depth were made near the rods of the grid established for topographic measurements (Figures 4.3 and 4.4). The contrasting sand was inserted near the rods, using 30 cm plugs. After the overwash event, during the next low tide, the exact sites where the plugs were placed were excavated to verify the distance from the plug to the surface. The topographic variations were obtained by the measurement of the rods before and after the overwash event.

4.2.1.5. Grain-size

Superficial sediment samples were collected during the GO.1 and GO.3 fieldwork campaigns. About 200 g of sediments were collected next to the rods of the topographic grids, before and after the overwash event. For GO.1 a sample was taken next to the rods that defined the cross-shore profiles 1, 3 and 6, until row G (Figure 4.3), totalling 38 samples, covering both the top of the beach and the washover plain. Because the tide was already rising during the sampling, some lower elevation sites were not sampled. For GO.3 samples were taken near the rods that define the cross-shore profiles 2 and 5 (Figure 4.4), from row A to G, totalling 28 samples.

4.2.1.6. Tracers

The sediment transport patterns were studied using fluorescent tracers (FT). The preparation of the FT consisted of collecting sediment from the study area, washing to eliminate salt, dying with orange fluorescent ink, and sieving to remove aggregates (following procedures described in Ciavola *et al.*, 1998). Before the fieldwork campaigns, samples were taken from the original sand and from the tracers.

For GO.1 the 40 kg of FT were placed at 00:30 February 10th 2001, forming a rectangle, as superficial as possible, on the top of the beach face, at about 1 m from the washover crest. For GO.3 the 42 kg of FT were dropped into the flow at the washover mouth, between 03:20 and 03:46, February 19th 2003.

After the overwash event finished shallow corers were manually taken, using 35 mm diameter PVC tubes about 50 cm long. The obtained corers, that mostly had about 25 cm depth, were opened at the field site and sub-sampled every 5 cm. The main limitations of the corer technique were: (1) the proximity to the water table, which prohibited the coring of the lower parts of the beach; and (2) the existence of coarse sand at the base of the core, which limited the depth of sampling. During GO.1 the corers were taken near each rod of the grid (except row I, Figure 4.3), totalling 41 corers, and 223 samples. During GO.3 it was considered that the defined grid on the washover (profiles 1 to 3, rows A to D, Figure 4.4) was not sufficiently representative, and therefore 17 extra corers were added, in irregularly spaced radial transects on the washover fan. From the GO.3 fieldwork a total of 31 corers and 135 samples were obtained.

4.2.2. DATA PROCESSING AND LABORATORY PROCEDURES

4.2.2.1. Forcing mechanisms

The PT data from the ocean side of the barrier were processed in two different ways: a) to obtain the tide level, and b) to obtain wave parameters. The PT sensor with the lowest elevation was used for wave and tide computations, i.e., PT6 for GO.1 (Figure 4.3) and PT5 for GO.3 (Figure 4.4).

To determine the tidal elevation the atmospheric pressure was firstly subtracted from the pressure records and this water pressure was then converted to water depth. The data was

then grouped into 10-minute blocks and the average water depth of each block was calculated. The average water depth for each block was added to the sensor height above the datum to provide the tidal height on the ocean side of the barrier.

The wave parameters used for this study were the significant wave height at breaking (H_{sb}), maximum wave height (H_{max}), and peak period (T_p). The wave parameters were calculated using spectral methods (i.e. method of moments) after first using a spectral weighting function to compensate for attenuation due to water depth.

The data collected by the PT located on the lagoon side of the barrier was used for tidal level computations. The procedures were similar to those described for the seaside PT, except that the lagoon pressure data was collected in 1-min bursts, and the obtained water level curve was afterwards smoothed with moving averages of 5 points.

4.2.2.2. Overwash flow

The PT located at the top of the beach face were used to estimate overwash conditions. The 4 Hz pressure data were converted to water depth and split into blocks of 10 minutes. During fieldwork some observations were made: (1) beginning and end of the overwash event, (2) beginning and end of complete overwash flows, and (3) number of overwash flows/time. The comparison between field observations and the records of the PT located at the top of the beach allowed the definition of the conditions at which overwash can occur. For each water passage over the PT sensor on the top of the beach there was a record of a peak in water depth. However, not all run-ups that reached the top of the beach produced overwash flows. Therefore, the threshold conditions had to be established defining the amount of water depth variation (dh) that was required to produce an overwash flows (OF). The variation in water depth that was recorded for the first overwash flows (dh_1) and last overwash flows (dh_n) of the overwash event defined this threshold.

If $dh_x > dh_1 \approx dh_n$, then overwash flow occurs, where x is a single water depth variation over the sensor.

For complete overwash to occur higher water depth variations over the PT are required. The definition of the threshold for the complete overwash flow was defined as the water depth variations recorded for the first observed complete overwash (dh_{1+m}, m flows after the first overwash), and the last complete overwash (dh_{n-p}, p flows before the last overwash).

If $dh_x > dh_{1+m} \approx dh_{n-p}$, then complete overwash flows occurs.

For every 10-min block the number of overwash flows and complete overwash flows was determined. Because field observations of the number of overwash flows/time were made, a verification of the defined threshold was made.

The time measurements of the progression of the overwash front (GO.3) were used for the determination of the velocity of the overwash flow, using the distance between washover channel rods. The overwash velocity range was determined but the determination of detailed variation of the overwash flow velocities through time was not possible since measurements were neither systematic nor extensive.

4.2.2.3. Topography

Data collected with total station (GO.1) did not required further processing. Data collected with RTK-DGPS (GO.3) required some post processing in order to obtain data with a spacing of some 1.5 m; the smoothing of the data was made by averaging every 4 to 5 points. Geo-referenced data is referred to the Portuguese Melriça Grid, a recti-linear UTM co-ordinate system, and vertical heights were calculated in relation to MSL.

For all topographic surveys (two for GO.1 and two for GO.3), the cross-shore profiles were obtained from the survey and converted into distances from an arbitrary lagoon origin. Analyses were made with the comparison of pre-overwash with post-overwash profiles.

Volume computations per linear meter of coastline were made for all profiles, using the kriging method with a linear variogram to interpolate the upper surface and using the MSL as base line.

4.2.2.4. Mixing depth

The mixing depth was determined by the combination of two types of field measurements: the distance between the post-overwash topography and the coloured plug after excavation, and the variations of the topography. In cases of no topographic variations (equilibrium conditions) or accretion, the depth at which the coloured plug appeared was considered the mixing depth. In the case of erosion, the depth was added to the topographic variation to estimate the total activation layer. However, this approach is only valid if there are no extreme erosion or accretion events (Ferreira *et al.*, 2000). During the fieldwork campaigns, the total erosion of the coloured sand or the total burial of the reference rod did not occur.

4.2.2.5. Grain-size

Grain-size analyses were made of the sediments collected during GO.1 and GO.3, and of the sand used as tracers, before and after painting. Traditional laboratory dry sieving procedures for unconsolidated clastic sediments were used for all samples. Sieving was done between –5.0 ϕ and 4.0 ϕ, with a 0.5 ϕ discrimination interval, thus using 20 sieves.

The classical grain-size parameters were determined (mean, sorting, skewness, and kurtosis) following the Method of Moments, using the computer program GRADISTAT (Blott and Pye, 2001).

4.2.2.6. Tracers

The sub-samples of the corers were washed to eliminate the salt and dried at 50^{o}C. The samples were weighed, and an aliquot of 20 g was obtained and spread as single layer sand on a black plate. The number of FT grains was visually counted in a dark room under UV light. The number of FT grains per 100 g of sample was then extrapolated in order to generate maps of FT distribution. A distribution map was obtained for each of the sampled depths (0-5 cm, 5-10 cm, 10-15 cm, 15-20 cm, 20-25 cm) of the GO.1 and GO.3 fieldwork campaigns. The definition of FT mass centroids was obtained by applying the Spacial Integration Method (SIM; Komar and Inman, 1970; Madsen, 1987) that is an average location of the FT cloud weighted by the mass of tracer at each position of the grid. The percentage of FT that is remaining on the sampling grid (named percentage of remaining tracer, PRFT, in Vila-Concejo *et al.*, 2004; and percentage of recovery e.g. in Madsen, 1987; Ciavola *et al.*, 1998), was estimated by the following relation:

$$PRFT = M_T \times 100/FT_{injected} \quad (4.1)$$

where M_T is the total mass of FT remaining in the study area (kg), which results from the sum of the FT mass in each layer (M_L). To obtain M_L, the method developed by Vila-Concejo *et al.* (2004) was used, that is defined by the relation:

$$M_L = V_{Ri}/V_S \times M_{Si} \quad (4.2)$$

where V_{Ri} is the representative volume of each sample (representative area × height of layer), V_S is the sample volume and M_{Si} is the mass of FT in each sample.

For the GO.1 and GO.3 fieldwork campaigns the representative area of each sample was considered to be the area enclosed by the polygon defined by the half-distance to every neighbour sampling point. At the sampling points forming the external boundary of the grid the polygon was constructed using the half-distance to the neighbours inside the grid and the joining of the external points of the grid, therefore smaller representative areas were

computed. The mass of FT was obtained by multiplying the number of FT grains in each sample by the sand density (assuming quartz sand) and the average grain volume (based on the mean grain-size).

4.3. RESULTS

4.3.1. FORCING MECHANISMS

During GO.1, the maximum oceanic tidal level was 1.71 m MSL (almost 10 cm below tidal predictions) reached at 03:30, February 10th 2001 (Figure 4.5a). The highest lagoon tidal level was 1.67 m above MSL, reached at 04:15 (Figure 4.5a). During GO.3, the maximum oceanic tidal level was 1.69 m above MSL (coincident with the tidal predictions), reached at 03:40, February 19th 2003 (Figure 4.5b). The highest lagoon water level was 1.67 m above MSL, reached at 04:20 (Figure 4.5b).

For both fieldwork campaigns the maximum ocean water elevation is very similar (around 1.7 m above MSL, corresponding to equinoctial spring tides), and almost coincident with the lagoon water levels. However, there is a lag of 45 minutes for GO.1, and 50 minutes for GO.3 between the oceanic and the lagoon high tide slacks (Figures 4.5a and 4.5b). For both GO.1 and GO.3, it was noticed that the ebb tide is faster on the oceanic side than on the lagoon side, thus the lagoon water maintained relatively higher levels for a longer time.

The wave height at breaking (H_{sb}) was somewhat variable during fieldwork (Figure 4.6) because the instruments were located inside the beach system, and therefore the recorded waves were greatly influenced by the nearshore bathymetry. For both fieldwork campaigns, the breaking point was located on the low tide terrace/ebb delta at low tide, and at the steep beach face, during high tide.

(a)

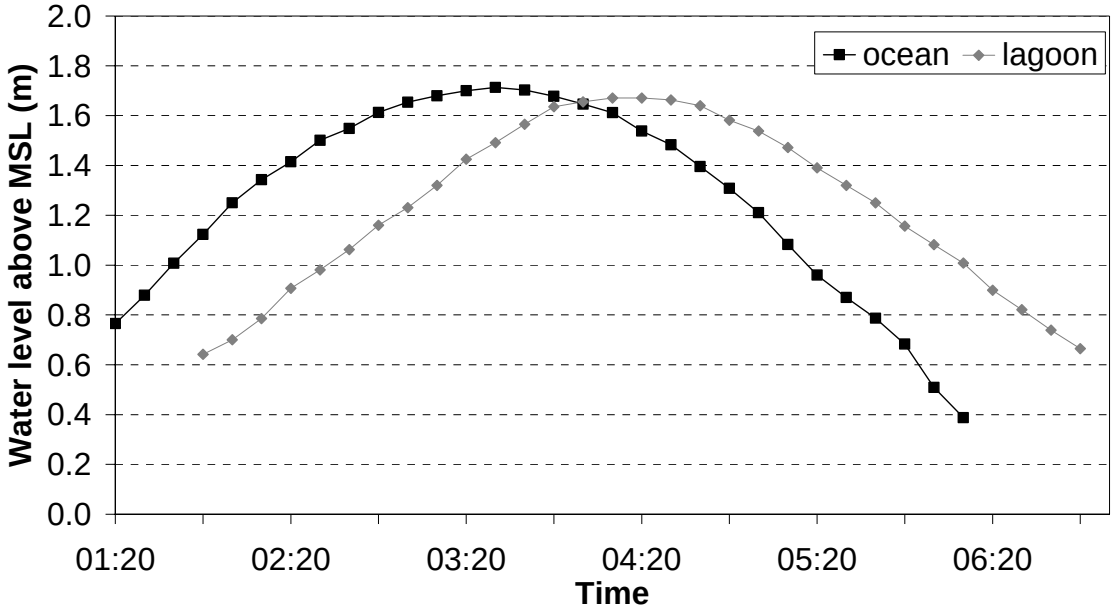

(b)

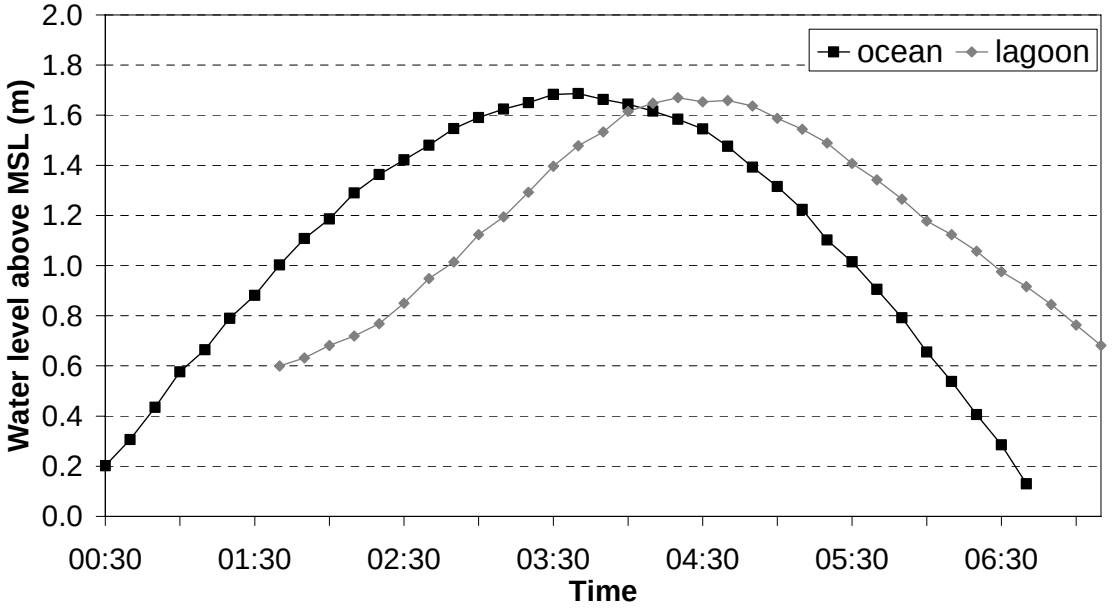

Figure 4.5. Tidal levels for oceanic and lagoon waters: (a) for GO.1, and (b) for GO.3.

The average values for the wave parameters were calculated considering only the high tide records (GO.1 from 02:00 to 04:00, and GO.3 from 03:10 to 04:10), when there was a slight stabilisation of the parameters (Figure 4.6). Average H_{sb} for GO.1 was 1.28 m, average H_{max} was 2.76 m, and average T_p was 11.1 s. For GO.3, the average H_{sb} was 1.21 m, the average H_{max} was 2.86 m, and average T_p was 16.0 s. The waves were relatively similar

during both fieldwork campaigns, however GO.3 waves had longer period and thus likely to be more affected by nearshore bathymetry.

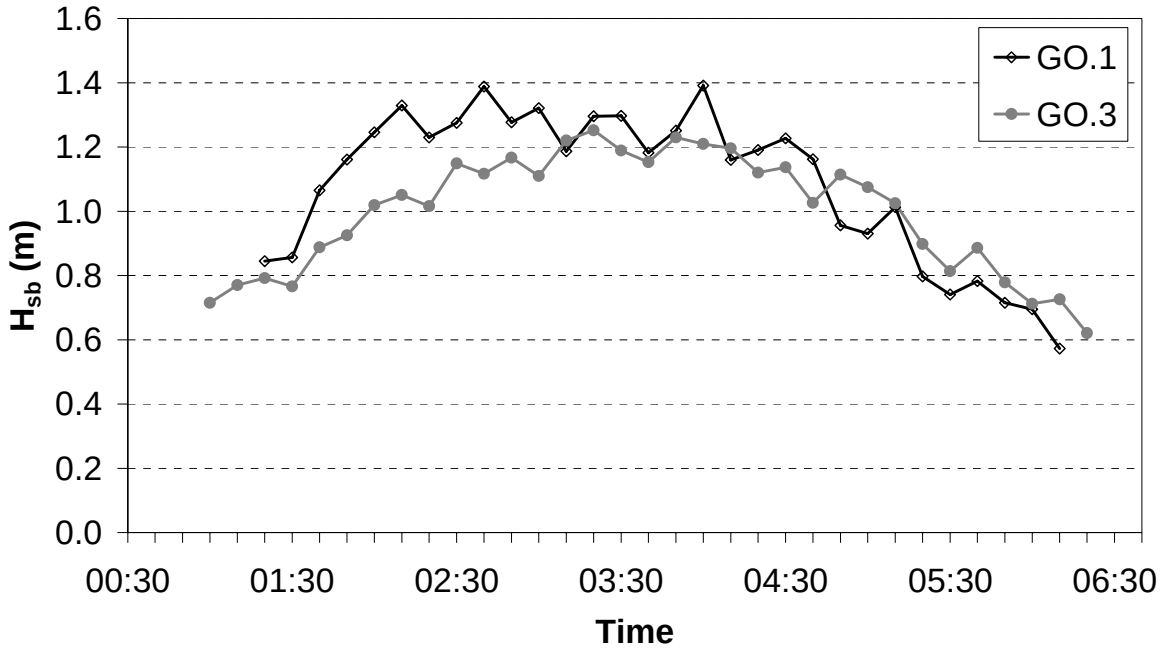

Figure 4.6. Variation of significant wave height at breaking (H_{sb}) during GO.1, and GO.3 fieldwork.

4.3.2. OVERWASH FLOW

During the fieldwork campaigns, *in situ* observations were made of the swash and overwash, which allowed a characterisation of a succession of stages during the tidal cycle. The overwash event during the GO.1 fieldwork started at 01:27 and finished at 06:02, February 10th 2001, with complete overwash occurring between 02:10 and 04:54. The overwash event during the GO.3 fieldwork started at 01:59 and finished at 05:27, February 19th 2003, with complete overwash occurring between 02:44 and 04:39. The event started with waves breaking under high-tide conditions generating swash moving up the beach face. The generated run-up flow reached the washover crest or mouth as a shallow sheet of water with decreasing velocity. On other occasions it was the combination of the waning stage of the run-up with a second swash event from a wave breaking shortly after that generated a

sufficiently higher elevation run-up to reach the washover crest or mouth. Initially, the run-up reached the washover crest/mouth without generating an overwash flow, because of infiltration and backwash. As the tide continued to rise and the breaking point got closer to the washover, the swash induced flow reached the crest/mouth with sufficient momentum to generate a down slope flow over washover and the overwash event began. In general, for overwash flows on a washover crest (like in GO.1 and in parts of the study area of GO.3) the flow decelerated across the gently landward dipping terrace. Additionally, for overwash flows in a washover mouth (like in parts of the study area of GO.3) the flow accelerated in the steep restrictive channel and decelerated when it reached the fan. As the tidal level rose, it sometimes occurred that overwash flow reached the lagoon side of the barrier. At this stage, the waves were breaking close to the washover, the run-up was reaching the washover crest/mouth with high momentum and the duration of overwash of the crest/mouth was long. As a consequence, the overwash was flowing on the terrace or channel as a shallow unidirectional sheet of water with relatively high velocities and the overwash maximum intrusion was reaching the washover terminus or the steep end of the washover fan. During the ebb tide, the same stages occurred but in reverse order, with the end of complete overwash, the end of the overwash event, and subsequently decrease in run-up levels such that the washover crest/mouth were not reached.

The records of the PTs located near the washover crest/mouth, coupled with the field observations provided an estimate of the overwash threshold conditions as described in section 4.2.2.2. For GO.1 it was determined that overwash occurred when the variation of water level (dh) were higher than 10 cm and complete overwash occurred when dh was higher than 50 cm. For GO.3 it was determined that overwash occurred when $dh > 4$ cm and complete overwash occurred when $dh > 50$ cm. For each 10 min block the number of overwash and complete overwash was counted (see Figure 4.7a and 4.7b as examples).

(a)

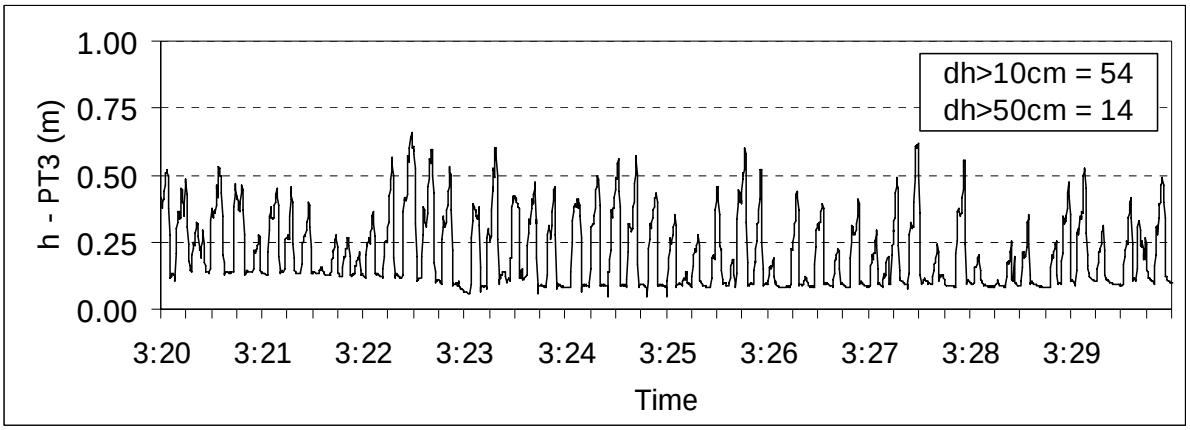

(b)

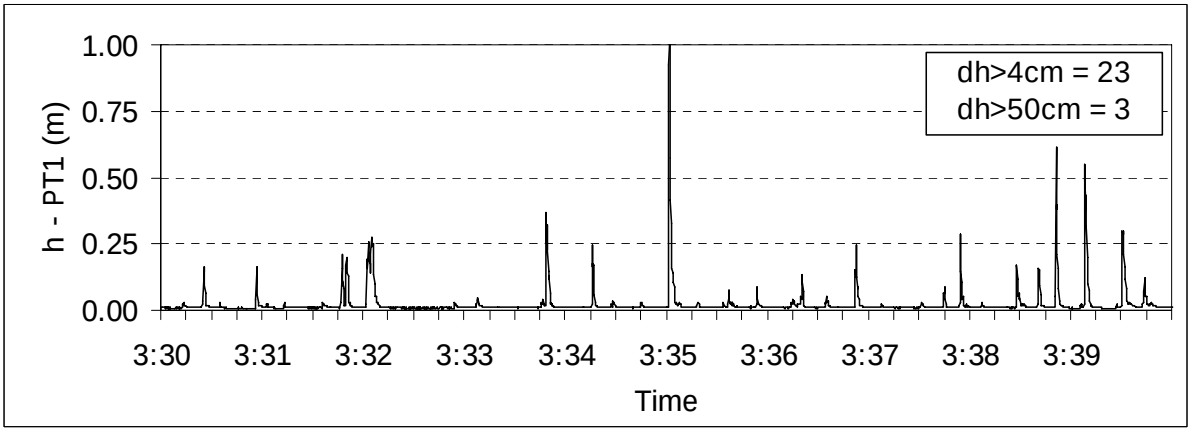

Figure 4.7. Example of a 10-min block of the water height above sensor (h-PT) of (a) GO.1, and (b) GO.3, and the indirect counting of overwash flows.

There is a variation in the number of overwash as a consequence of the variation of the tidal level (Figure 4.8a and 4.8b). The duration of the overwash event was about 4.5 hours for GO.1, and 3.5 hours for GO.3. The estimated total number of overwash flows was very different from GO.1 (915 occurrences) to GO.3 (280 occurrences). The estimated number of complete overwash flows is more contrasting, with GO.1 (152 occurrences) having about 8 times more than GO.3 (20 occurrences). Approximately the same number of overwash flows occurred before (48% for GO.1 and 54% for GO.3) and after the high tide slack, for both fieldwork campaigns. However, the complete overwash flows of GO.3 occurred preferentially before the high tide slack (83%), while the complete overwash flows of GO.1 were distributed equally before and after high tide slack (Figures 4.8a and 4.8b). For the GO.1 fieldwork, at the high tide slack the overwash period was very similar to the wave peak period (about 11 s),

while for the GO.3 fieldwork the overwash period was 26 s to 46 s and wave peak period was about 17 s.

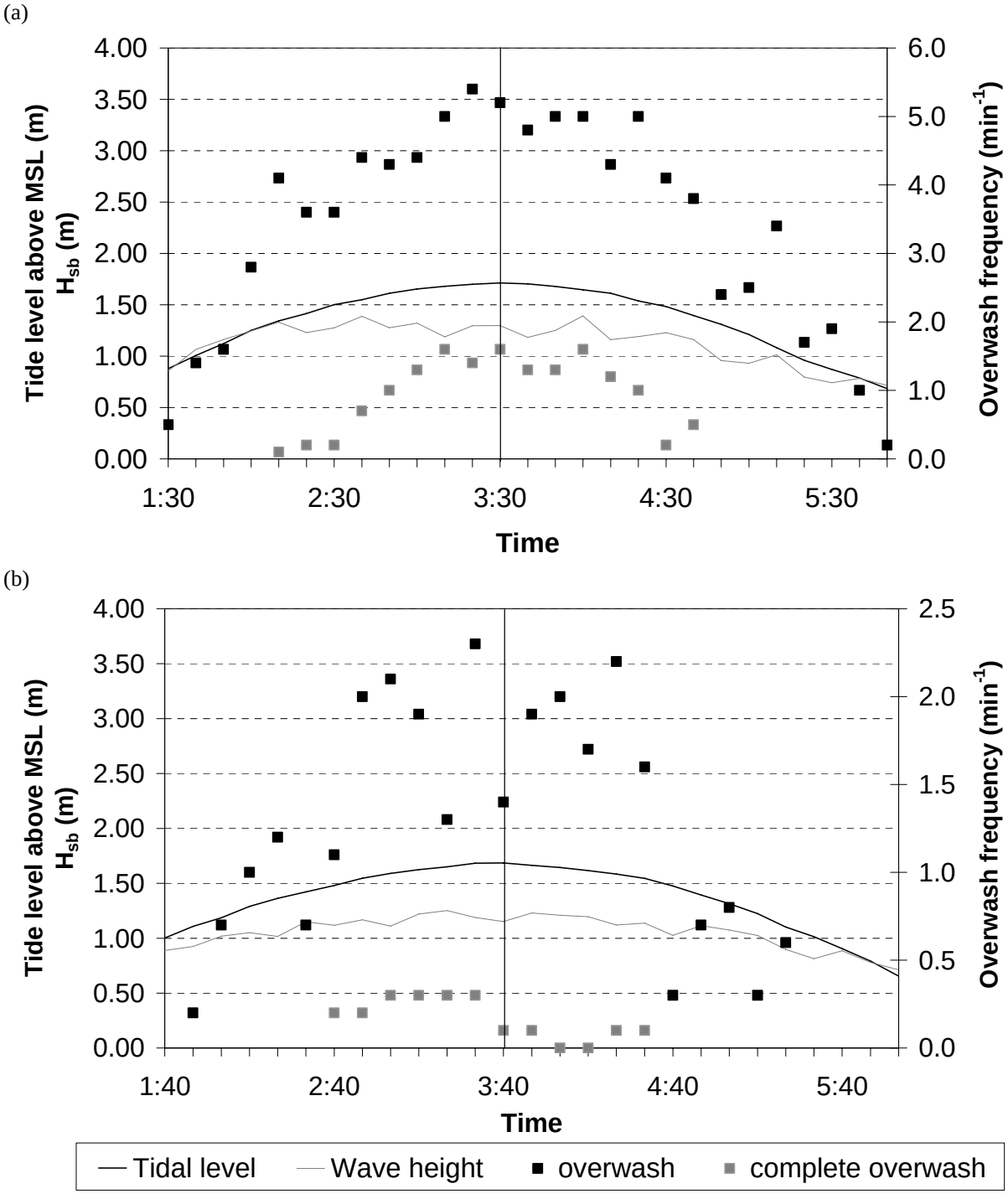

Figure 4.8. Frequency of overwash and complete overwash (right axis), tidal levels and significant wave height (left axis) for (a) GO.1, and (b) GO.3.

The overwash flow velocities measured between rods during the GO.3 fieldwork varied between 0.9 m/s and 5.7 m/s, however the most frequent velocities range between 2.5-3.0 m/s

(Figure 4.9). These measurements corresponded to the more developed flows; however there were a great number of overwash flows that were not measured because they had smaller intrusion distances and did not reach the second rod of the measurements. Therefore, the average overwash flow velocity is probably overestimated by the above mentioned velocity measurements.

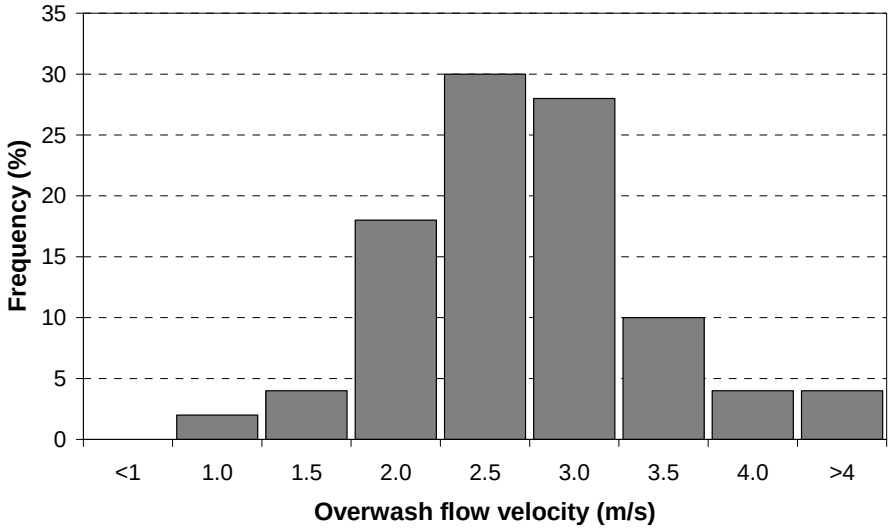

Figure 4.9. Frequency of overwash flow velocities for GO.3 fieldwork.

The indirect measurements of the overwash maximum intrusion through the tracer shell placement, undertaken during GO.1, had the problem of the low amount of shells found on the field site. The number of shells counted (about 1% of the placed marked shells) was not enough to generate a distribution map. On the washover mouth, central channel and main central fan almost no tracer shells were found. The high elevation of the central fan together with the lateral spreading of the overwash flow generated lateral secondary smaller dimensions half-fans. The tracer shells that were found were mainly located on these lateral half-fans, both near the washover channel and at distal top surfaces. Field observations point to the possibility of marked shells transport to the distal fan, below lagoon water level. It is also possible that the sand deposited by overwash flow buried the marked shells.

4.3.3. MORPHOLOGIC VARIATIONS

The six cross-shore profiles measured before and after the overwash event of the GO.1 fieldwork, showed relatively similar morphologic variations. The greatest variation occurred on the washover crest, where an overall accretion of about 16 cm of sand occurred (Figure 4.10). The accretion was wedge shaped, with a null point located above lagoon high tide level, below which the small variations (generally less than 10 cm) can be attributed to the lagoon currents. The wedge-shaped accretion mostly occurred until 04:00; after which time very small morphologic variations were noticed (Matias *et al.*, 2003). During the overwash event there was vertical accretion over the washover crest, but no horizontal landward progradation was noticed. The average volume variation in the study area was approximately +3.4 m^3/m.

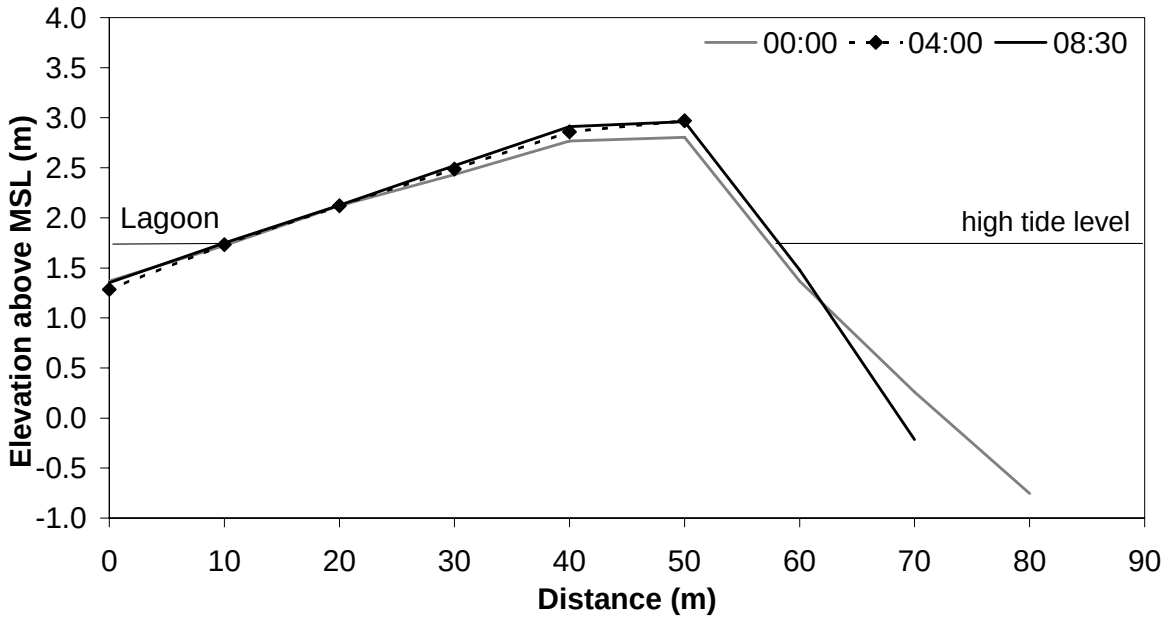

Figure 4.10. Washover plain morphologic variations for an average cross-shore profile (profiles 1 to 6 of Figure 4.3), during GO.1 fieldwork campaign.

During the GO.3 fieldwork, the two types of washovers registered two different morphologic changes. The washover lobe central profile showed erosion on the mouth and channel, and accretion on the fan (Figure 4.11a).

(a)

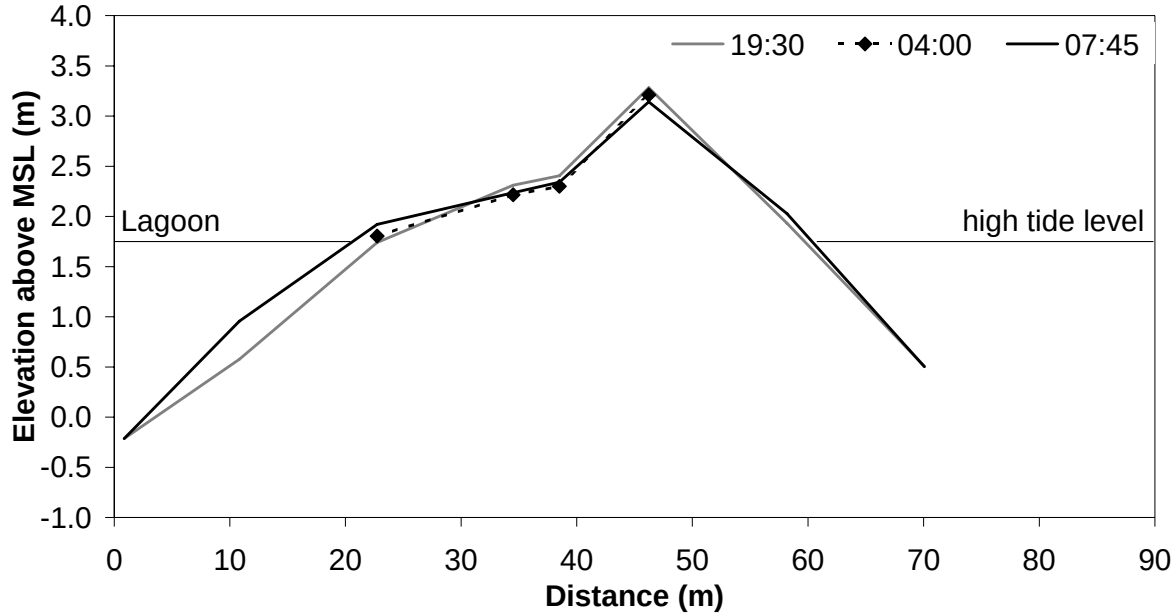

(b)

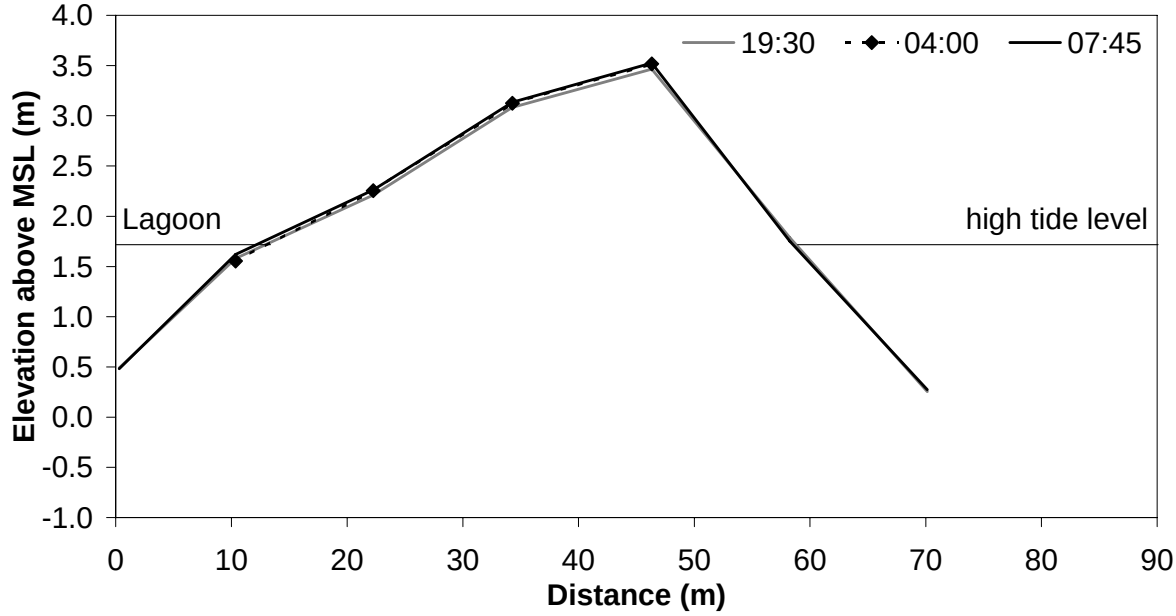

Figure 4.11 Morphologic variations during GO.3 fieldwork for cross-shore profiles: (a) washover lobe central profile, and (b) washover plain average profile (profiles 4 to 6 of Figure 4.4).

The washover plain average cross-shore profile had accretion starting on the crest until near the lagoon high tide level, similarly to the GO.1 washover plain (Figure 4.11b). On the washover lobe, some morphological changes were noticed, after 04:00, especially the erosion of the mouth and deposition on the fan. On the washover plain, after the high tide slack, almost no changes occurred, similarly to what occurred on the GO.1 washover plain. During the GO.3 overwash event there was mainly a small vertical accretion on the washover plain, and a horizontal landward progradation on the washover fan. The volume variation of the central lobe profile was +4.7 m^3/m, while the average volume variation of the profiles on the washover plain was +1.3 m^3/m.

4.3.4. MIXING DEPTH

For both fieldwork campaigns mixing depth was determined for every node of the sampled grid, and distribution maps were made (Figure 4.12a and 4.12b). The mixing depths determined for the entire study area of the GO.1 fieldwork varied from 4 cm to 51 cm, with an average for the washover plain of about 13 ± 7 cm. There was a global distribution of the mixing depths in longshore bands, diminishing from the beach to the interior parts of the washover terrace (Figure 4.12a). The beach face showed the greatest mixing depths (average of 25 cm) and the interior parts of the washover terrace had the smallest depths (average 8 cm). The crest was the part of the washover that showed the greatest mixing depths (average 18 cm), but the terminus of the washover also had a relatively deep layer of disturbed sediments (average 15 cm).

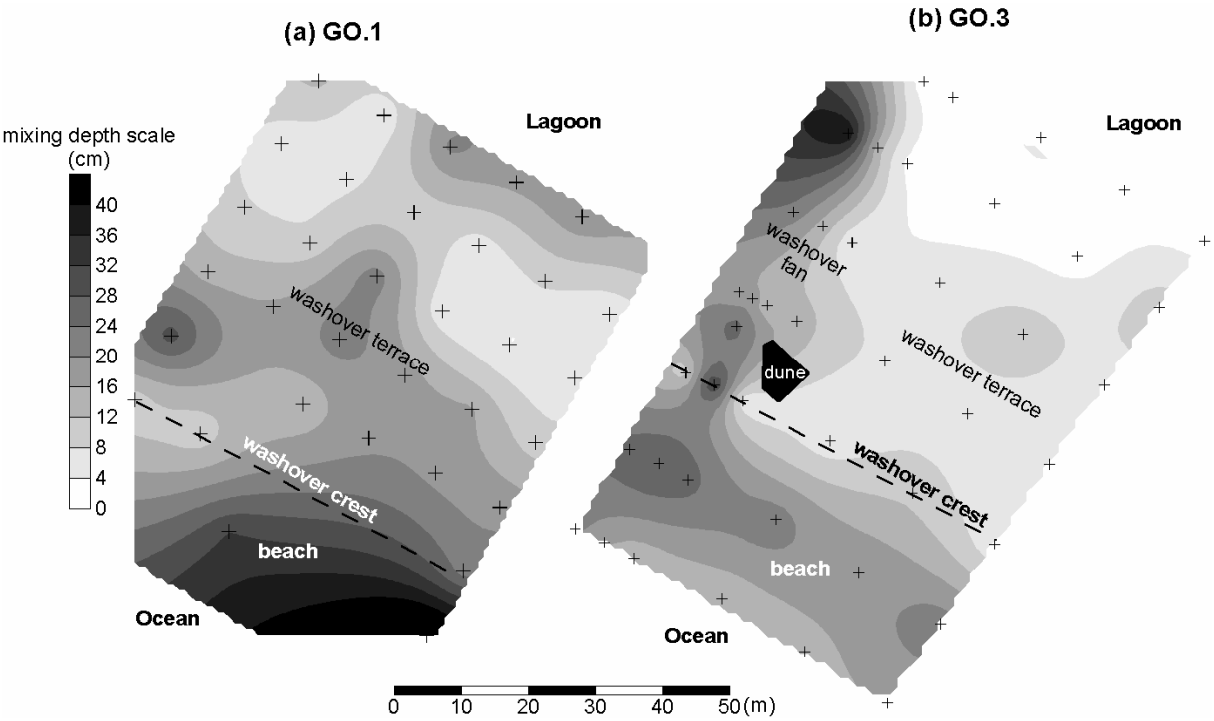

Figure 4.12. Mixing depth distribution in the study area for (a) GO.1, and (b) GO.3.

For the GO.3 fieldwork, the mixing depths had distinct values and distribution for the washover plain (average 6 ± 3 cm) and the washover lobe (average 15 ± 11 cm). The mixing depth for the entire study area varied between 41 cm and 1 cm. The beach face had an average mixing depth of about 20 cm, which corresponds to the highest average values. The washover lobe varied from an average of about 16 cm at the mouth, increasing to an average of about 18 cm in the channel, and again decreasing in average to the fan (13 cm). At the washover plain, the crest and the terrace had almost the same values (average about 7 cm), decreasing to the washover terminus to an average of about 4 cm.

4.3.5. GRAIN-SIZE

The grain-size analysis of the sediments collected during the GO.1 and GO.3 fieldworks is summarised in Table 4.1. The details and interpretation of the grain-size analysis of these fieldwork campaigns and other samples collected in the study area can be found chapter 6.

The beach face sediments are generally dominated by moderately to well sorted coarse sand, with almost no gravel or fine sand contents. Generally, the washover crest/mouth sands were similar to the beach sediments but had an increase in gravel and fine sand. The washover plain has a tendency for increase in mean grain size with the distance to the crest. The washover terminus or fan distal steep surface had the coarser mean grain size of the sampled area (Table 4.1).

Table 4.1. Average values of mean grain-size and sorting for the samples located on the beach and washover, and for the sand before and after dying (FT).

	GO.1		GO.3	
	Mean (ϕ)	Sorting (ϕ)	Mean (ϕ)	Sorting (ϕ)
Beach face	0.89	0.75	0.31	0.34
Washover crest	0.72	0.73	0.52	0.46
Washover terrace	0.32	0.70	0.30	0.60
Washover terminus	-0.10	0.74	0.07	0.83
Sand before dying with paint	0.63	0.57	0.88	0.53
FT	0.41	0.50	0.52	0.57

4.3.6. SEDIMENT TRANSPORT PATTERNS

The transport of the 40 kg of tracer during GO.1 began at 00:43 on February 10th 2001. The FT distribution maps of GO.1 point to two main areas of sand transport, one landward of the injection point and another near the SE end of the sampling grid (Figure 4.13). However, the higher FT counting was next to or at a small distance landward from the injection point. About 57% of the FT counted in the laboratory was in the layers 10-15 cm and 15-20 cm, and only about 4% were in the deepest layer (20-25 cm).

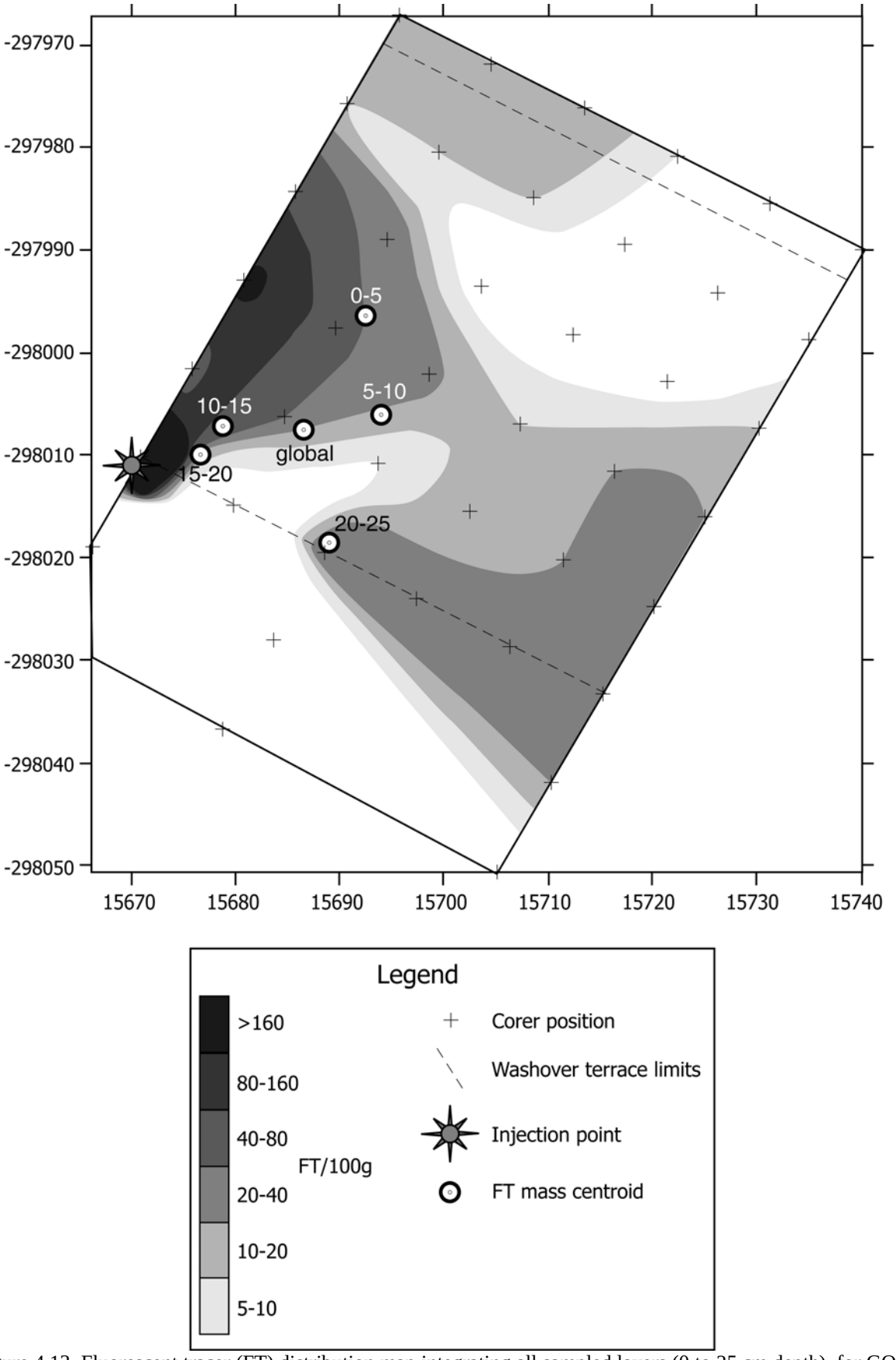

Figure 4.13. Fluorescent tracer (FT) distribution map integrating all sampled layers (0 to 25 cm depth), for GO.1 fieldwork. The mass centroid location is also represented, both for each of the sampled layers (0-5 cm, 5-10 cm, 10-15 cm, 15-20 cm, and 20-25 cm depth), and for the sum of all layers (global).

The mass centroid positions constitute an estimate of the average transport distance for each of the layers. The deepest layer (20-25 cm) shows a displacement in relation to the injection point that is dominated by the longshore downdrift component, yet in the superficial layer (0-5 cm) the average FT transport is dominated by the cross-shore landward component (Figure 4.13).

For the computation of the remaining tracer (PRTF of equation 4.1), the total study area (3,300 m^2), was irregularly divided into 41 polygons that define the representative area of each sample. The area of the polygons multiplied by the layer height (0.05 m) provided the representative volume (V_{Ri} of equation 4.2). The volume of the sample (V_S of equation 4.2) was 48 mm^3, and was constant for all samples because they where all obtained with the same diameter corer (35 mm). The mass of FT in each sample (M_{Si} of equation 4.2) was calculated by multiplying the counted grains/sample for the estimated weight of a FT grain. For this, the mean grain size of 0.41 ϕ (Table 4.1) was converted into mass, assuming that all FT grains were quartz (2650 kg/m^3). The application of equations 4.1 and 4.2 to GO.1 FT data allowed an estimate of about 68% for PRTF.

The FT distribution maps of GO.3 showed a progressive displacement of the FT cloud landward, from the deepest layers (20-25 cm, Figure 4.14e) to the superficial layer (0-5 cm, Figure 4.14a). The mass centroids also showed a general increase in landward displacement for the superficial layers. In some layers (0-5 cm and 10-15 cm) there was FT transport to the adjacent washover plain, however the highest concentrations were located on the top of the washover fan belonging to the washover lobe (Figure 4.14). The layer that had the highest count was the deepest (20-25 cm), with the two superficial layers (0-5 cm and 5-10 cm) accounting for only 18% of the count.

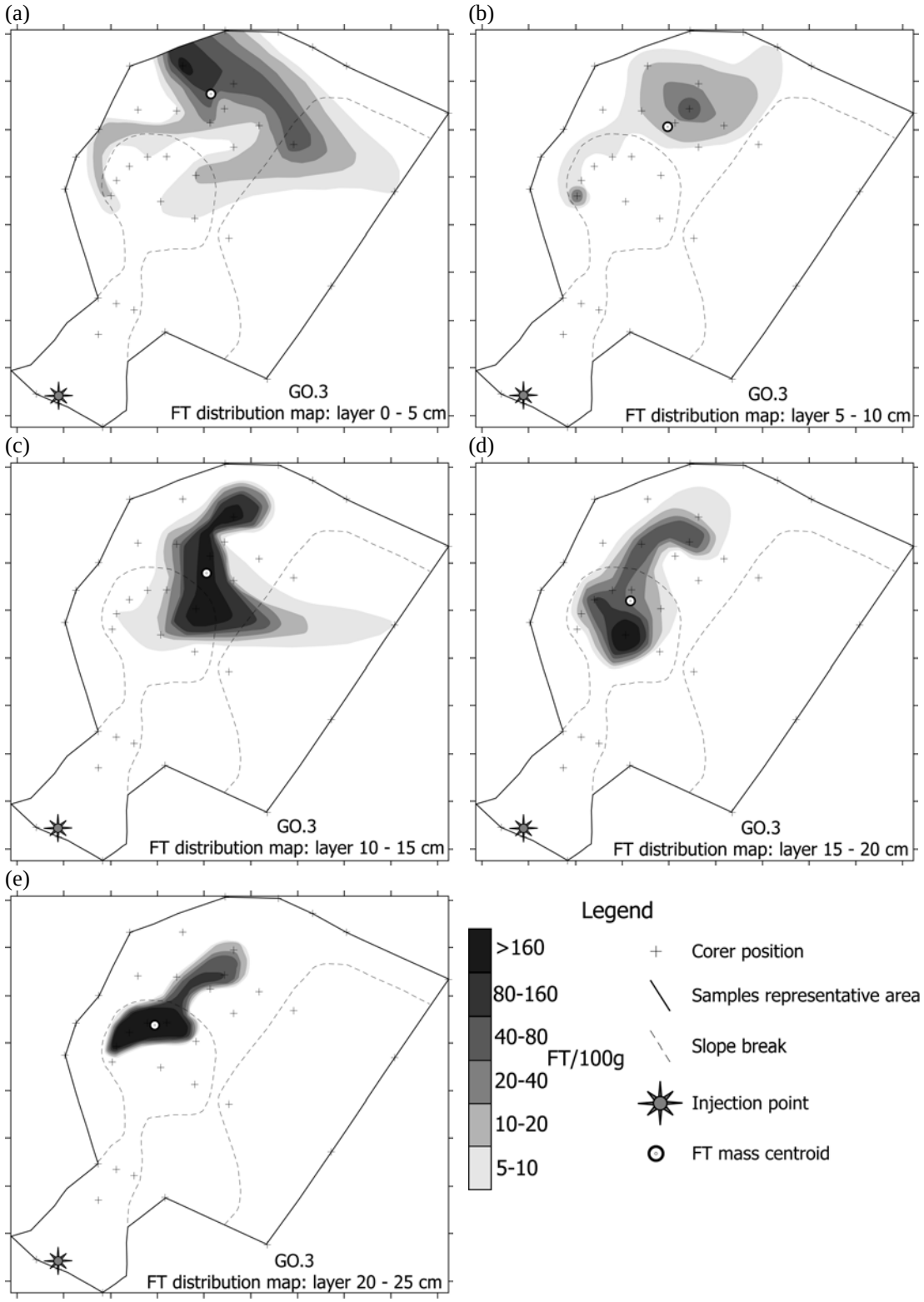

Figure 4.14. Fluorescent tracer (FT) distribution map for all sampled layers, for GO.3 fieldwork: (a) 0-5 cm, (b) 5-10 cm, (c) 10-15 cm, (d) 15-20 cm, and (e) 20-25 cm depth. The mass centroid location of each layer is also represented.

The computation method of the remaining tracer (PRTF of equation 4.1) for GO.3 was the same as for GO.1. The total study area is smaller, about 1,040 m^2, but the number of

polygons was similar (38 polygons). The area of the polygons multiplied by the height layer (0.05 m) provided the representative volume (V_{Ri} of equation 4.2). The volume of the sample (V_S of equation 4.2) was the same as GO.1 since the same coring technique was used. For the determination of the mass of FT in each sample (M_{Si} of equation 4.2) the same method was used, but a mean grain size of 0.52 ϕ (Table 4.1) was used. The application of equations 4.1 and 4.2 to GO.3 tracer data allowed an estimate of about 77% for PRTF.

4.4. DISCUSSION

4.4.1. WASHOVER SHORT-TERM DYNAMICS

The two fieldwork campaigns described above recorded overwash events under similar oceanographic conditions (Figures 4.5 and 4.6) with moderate (non-storm) wave energy and spring high tidal levels. Therefore, the differences in sediment transport observed during the fieldwork campaigns are mostly related to the morphologic characteristics of the washovers. The comparison between the morphologic variations of GO.1 and GO.3 showed that the washover plains of the two different fieldwork campaigns behave more alike than contemporary washovers of different types (lobe *versus* plain). Consequently, the overwash processes that were observed on washover plains are discussed separately from those observed on washover lobes.

4.4.1.1. Washover plain dynamics

The washover plains that were studied had similar cross-shore profiles, even though the crest elevation was different. The shape of the washover plain was of a convex featureless surface, gently dipping landward (Figures 4.10 and 4.11b). The washover crest marks the transition between the top of the beach and the washover terrace, and had an asymmetrical cross-sectional profile with a steep side facing seaward (slope of about 0.14) and a gentle slope side facing landward (slope of about 0.03, Figures 4.10 and 4.11b).

During the overwash event, both GO.1 and GO.3 washover plains showed accretion as a thin sandy layer (Figures 4.10 and 4.11b). The accretion volumes were different (3.4 m^3/m for GO.1 and 1.3 m^3/m for GO.3), which was probably related to the average crest elevation (2.8 m for GO.1 and 3.5 m for GO.3). Under the same oceanographic conditions, and similar

shoreface, the higher crested washover plains were overwashed for a shorter interval, thus showing that the difference in washover crest elevation was the critical parameter for overwash occurrence. It was found that the overwash flows on washover plains were constructive (see section 4.3.3), and that the differences between the accretion volumes were directly related to the amount of overwash flows, being higher for more intense overwashing. Under these circumstances, the type of accretion deposit was a wedge-like thin layer of sand, denoting a decrease in flow capacity as it progresses through the surface. The mixing depth for both plains showed that the active layer for the interior parts was very shallow (Figure 4.12). This means that the net small morphologic variations were not the result of oscillatory morphological changes, i.e., successive erosion and accretion processes. On both washover plains the crest was the most dynamic part, with accretion taking place as a consequence of the drop in flow capacity as the overwash overcomes the crest and flows over a gently landward dipping surface. Therefore, the convex crest shape was a very significant factor in retarding the flow progression.

The coarsening of the sand mean grain-size in the direction of the overwash flow transport (Table 4.1) was apparently contradictory to the loss of flow competency. However, this coarsening was probably due to a relative increase in shells content because of their higher transportability and deposition near maximum intrusion lines (Chapter 6).

The sediment transport patterns obtained with tracers for GO.1 showed that during the early stages of overwash, when the intrusion was relatively small, the upper beach face and the washover crest were in sedimentary connection. The sediment transport in this stage had an important longshore component (mass centroid of layer 20-25 cm, Figure 4.13). As overwash frequency increased the onshore sediment transport became more significant. The patterns show that there was very small longshore transport of the tracer, thus suggesting that the flow induced transport was dominantly shore-normal. The longshore displacement of the

mass centroids in relation to the injection point (especially mass centroid of layer 5-10 cm, Figure 4.13) was due to the early tracer transport at the upper beach face before entering the washover plain. The relatively small onshore transport, with a high concentration of tracer near the injection point, was due to the constructive processes that occurred at the washover crest (see Section 4.3.3) by which the tracer was buried by the continuous arrival of beach sand at the top of the beach face.

According to the integrated analysis of the morphologic data, mixing depth distribution, and tracer transport, the sediment movement on the washover plain during an overwash event can be divided into three main stages: Stage 1 - Crest Accretion, Stage 2 – Onshore Transport, and Stage 3 - Dynamic Equilibrium. At the beginning of the overwash event, the wave run up starts to overtop the washover crest. Because the crest had a gentle landward angle, the progression of the flow was inhibited and the sedimentary processes were similar to the ones occurring at beach berms, and that were defined by crest overtopping by Orford and Carter (1982). The washover crest was contiguous to the top of the beach and the sand transported by the run up over the beach face was generally deposited at this perched transitional morphology (Stage 1). The rise in the tide level induced not only an increase in overwash frequency but also an increase in overwash flow intrusion, until complete overwash started to occur, thus starting Stage 2 (Figure 4.8a). During Stage 2, the overwash flow was more rapid with the seawater constantly overtopping the crest. The flow over the plain had the capacity to transport sand up to a variable distance according to the overwash intrusion. Almost all the transport and associated morphological changes occurred before the high tide slack (Figures 4.10 and 4.11b). Once the tide started to drop, even while similar overwash frequencies were maintained (Figure 4.8a), the morphological changes became negligible (Stage 3). In this way, for washover plains, there is an asymmetrical behaviour due to the fact that Stages 1 and 2 induced most of the morphological changes before the high tide slack and Stage 3, after the

high tide slack, showed morphologic stability. It seems that there was an adjustment of the sedimentary environment to the initial unbalance induced by the beginning of the overwash event (Stage 1) and following this to the higher magnitude overwash at the high tide slack (Stage 2). Subsequently, the lower magnitude overwash did not rework significantly the washover plain and the dynamic equilibrium stage (Stage 3) was achieved.

4.4.1.2. Washover lobe dynamics

One washover lobe was studied during the GO.3 fieldwork. The washover lobe was distinct from the washover plain, not only in plan-view (Figure 4.4) with a distinct teardrop shape, but also in cross-shore profile (Figure 4.11). The mouth was very sharp and well defined (Figure 4.11a), marking the transition between the steep beach face (slope of about 0.11) and the steep washover channel (slope of about 0.11). Landward of the channel, the gently dipping slope of the washover fan ended in the prograding steep distal fan.

During the overwash event of GO.3, the cross-shore profile had significant morphological changes, especially erosion of the seaward washover morphologies (mouth and channel) and accretion of the landward morphology (washover fan distal surface, Figure 4.11a). The recorded accretion on the lobe central profile was +4.7 m^3/m, which was higher than the accretion measured on the washover plain of GO.1 that was overwashed more than 3 times more frequently than the GO.3 lobe. However, it must be stressed that the longshore volume variations on the washover plains were relatively uniform, unlike the lobes in which the variations were confined to the central parts. The determination of the mixing depth showed that the most dynamic parts were the washover mouth and distal fan that had similar or higher mixing depths than the beach face (Figure 4.12).

The mean grain-size was coarser for distal washover parts (Table 4.1) similar to what was observed for the washover plain. The tracer shells that were used during the GO.1

fieldwork on a washover lobe reinforce the possible explanation of the shells higher transportability. All tracer shells were transported into the washover fan, however, only a small percentage of the shells was found to be on the fan surface. Considering that the steep washover distal fan surface was accretional and that no corer samples were taken it seems likely that the sand transported by the complete overwash buried the shells or that they were transported into the washover distal fan below lagoon water level. The tracer shells found on the secondary lateral half-fans also testify to the deposition under declining flow velocities due to overwash spreading.

The sediment transport patterns obtained with the tracers showed the landward progression of the sediments entering the washover mouth (Figure 4.14). The deepest layers deposited during the early stages of overwash had mass centroids closer to the washover channel (Figure 4.14d and 4.14e) and the superficial layers show a mass centroid displacement towards the lagoon (Figure 4.14a and 4.14b). On certain occasions the sediments that entered the washover lobe mouth were transported as far as the adjacent washover terrace and terminus, because of lateral spreading and also due to the flood currents in the lagoon channel (Figure 4.14a and 4.14c). Unlike the washover plain, the sediment transport inside the washover lobe can be characterised by one onshore flow stage. However, this onshore flow did not cause the same changes in the lobe through time, nor the same type of changes as those registered in the plain.

The run up flow at the top of the beach face encountered the almost vertical foredune erosional bluff. Intense reflection occurred and slices of dune were eroded and fell over the beach face, inducing dune front retreat. In places where a washover mouth developed on the dune front the wave up-rush was converted into overwash flow as it overtopped the washover mouth (Figure 4.2). In places where the beach slope was gentler, the wave run-up was faster, thus overwash started sooner and was able to develop larger intrusions. The dune erosion, due

to wave-generated run up impingement, caused the deepening and enlargement of the washover mouth. Once the mouth was overwashed, the lateral restriction of the flow in the channel together with the steeper landward slope induced the increase of the flow velocity and the subsequent erosion. The depth of the flow was shallow because no obstacle existed to inhibit the free passage of the seawater, but the velocity was kept relatively high. The fast run-up velocity was converted into a shallow overwash flow with average velocities of about 2.5 to 3.0 m/s (Figure 4.9) that transported sand into the distal parts of the washover fan. The bottom friction and infiltration on the fan surface, together with a lateral spreading possibly due to the absence of dunes on the lagoon side of the barrier, induced a deceleration of the flow and the consequent sand deposition. It was noticed that the erosion of the washover channel only occurred until the end of the complete overwash event (about 04:30, Figure 4.8b), afterwards some small accretion was recorded (Figure 4.11a). At this time, the overwash intrusion was reduced and the flow stopped in the channel thus causing the deposition of the sand. The continuation of the erosion of the washover mouth after the high tide slack (Figure 4.11a) possibly provided sand for the channel deposition.

4.4.2. MAIN FACTORS GOVERNING NON-STORM OVERWASH

The oceanographic conditions for GO.1 and GO.3 fieldworks were similar (Table 4.2), both in terms of tides (oceanic and lagoon, Figure 4.5) and waves (Figure 4.6). The wave height corresponded to typical winter conditions in this area (1.0 to 1.5 m, Costa *et al.*, 2001). The submerged morphology was not measured but during both fieldwork campaigns was strongly dependent on the location and morphology of the Ancão Inlet ebb delta (see Figure 4.1 as an example). Also, the sub-aerial beach was similar during both fieldwork campaigns, with a steep beach face (Table 4.2) without berms or other beach profile features (Figures

4.10 and 4.11). The grain size was somewhat different, however the sampled washovers were in the typical range of sand textures found in this area (Chapter 6).

Table 4.2. Background conditions at the start and end of overwash interval, for the GO.1 and GO.3 fieldwork campaigns.

Fieldwork campaign	Background conditions	Start of overwash event	High tide slack complete overwash	End of overwash event
GO.1	Time (hh:mm)	01:30	03:30	06:00
	Ocean tide level (m above MSL)	0.88	1.71	0.68
	Lagoon tide level (m above MSL)	0.50	1.67	1.08
	Significant wave height (m)	0.86	1.30	0.70
	Average washover crest elevation (m above MSL)	2.80	2.97	2.96
	Beach face slope	0.140	-	0.148
GO.3	Time	01:50	03:40	05:20
	Ocean tide level (m above MSL)	1.11	1.69	1.10
	Lagoon tide level (m above MSL)	0.60	1.67	1.49
	Significant wave height (m)	0.93	1.15	0.90
	Average washover mouth elevation (m above MSL)	3.28	3.21	3.14
	Beach face slope	0.112	-	0.093

The main background condition that differs between the two fieldwork campaigns was the elevation of the washover crest of GO.1 and the washover mouth of GO.3. During GO.3 this elevation was about 48 cm higher at the start of overwash and about 18 cm at the end when compared to GO.1. This difference provided longer overwash events for GO.1, 60 minutes more of overwash, and 40 minutes more of complete overwash (Figures 4.8a and

4.8b). Thus, the limiting conditions for the start and end of the overwash under non-storm winter waves for the study area can be linked to the relation between the tidal level and the washover crest/mouth elevation (Z_{crest}). The start of overwash for GO.1 was when the tidal level was about 1.9 m below the Z_{crest}, while for GO.3 the tidal level was about 2.2 m below the washover mouth (Table 4.2). The end of overwash occurred when tidal levels were 2.3 and 2.0 m below Z_{crest}, for GO.1 and GO.3 respectively. Therefore, on average, the overwash occurred when the tide was about 2.1 m below the Z_{crest}, with 1 m waves. During GO.2 fieldwork, the washover crest was about 4.1 to 4.2 m high, the high tide level was 1.6 m and overwash did not occur, for similar wave conditions (H_o = 0.93 - 1.21 m). The predicted threshold (Z_{crest} - 2.1 m) was not achieved by some 40 cm. It should also be noted that during GO.2 there was a berm at the top of the beach face, and therefore the foreshore conditions for overwash to occur were altered in relation to the ones of GO.1 and GO.3.

The main factors leading to the occurrence of non-storm overwash in the study area are the non-storm winter waves, spring high tides, absence of beach berm and low elevation washover crest/mouth. Non-storm overwash may not take place if at least one of the following conditions occurs (Figure 4.15):

- ✓ Lower waves typical of summer conditions
- ✓ Neap tides
- ✓ Beaches with a well-developed berm
- ✓ High elevation washover crest/mouth

The defined oceanographic conditions interacting with appropriate foreshore morphologies can promote different non-storm overwash sedimentary processes (Figure 4.15):

✓ An unconfined overwash flow on the washover crest, with three evolutionary stages during the overwash event: Stage 1 (Crest Accretion), Stage 2 (Onshore Transport), and Stage 3 (Dynamic Equilibrium).

✓ A confined overwash flow in the mouth and channel, with a single stage during the overwash event, including mouth erosion, onshore sediment transport and fan deposition.

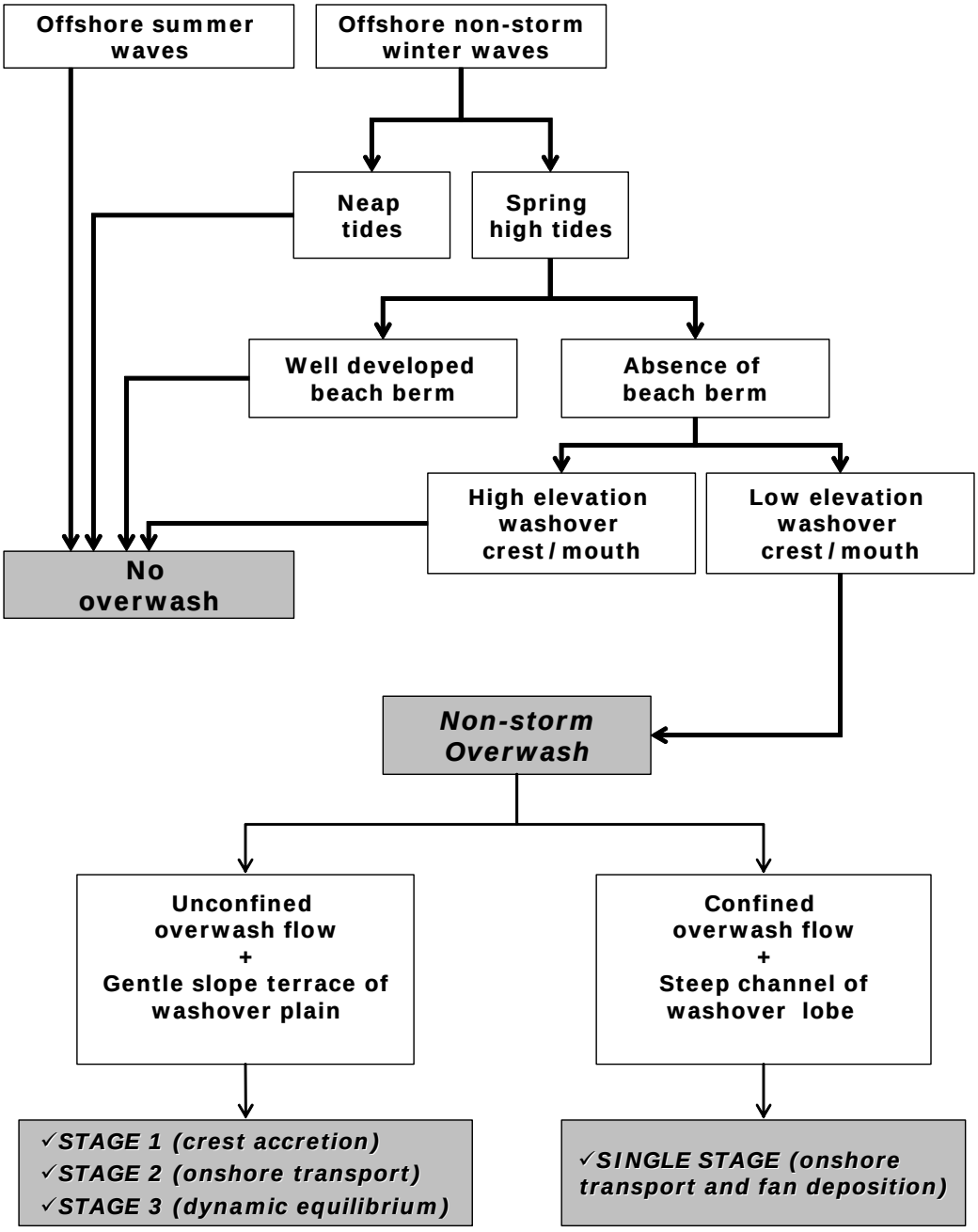

Figure 4.15. Factors governing non-storm overwash, and the sedimentary dynamics of washovers.

Although the main factors influencing overwash in the study area have been identified (Figure 4.15), they were observed to vary greatly both spatially and temporally. The wave climate has a seasonal behaviour, neap and spring tidal cycles promote variations in the high-tide elevation that occur twice a month, and the local bathymetry is very dynamic due to the nearby Ancão Inlet ebb delta and swash bars (Figure 4.1). The morphology of the study area also showed seasonal behaviour in response to the wave climate and was additionally influenced by the arrival of swash bars from Ancão Inlet (Vila-Concejo *et al., in press a*). On Barreta Island, washover lobes occur frequently, generating multiple dune features that once sufficiently close to each other frequently coalesce and evolve to form a washover plain.

4.4.3. NON-STORM OVERWASH IMPORTANCE

The overwash measured during the GO.1 and GO.3 fieldwork campaigns correspond to non-storm overwash events. The storm waves that usually are the driving mechanism for overwash occurrence on barrier dunes were not crucial since the spring high tide coupled with typical winter waves and a low-elevation barrier provided the necessary conditions.

During GO.1, the crest rose about 16 cm and an accretion of about +3.4 m^3/m was recorded. Most of these changes started when the tidal level was about 1.2 m, and complete overwash started when the tidal level was higher than 1.5 m MSL. Overwash was occurring during the high tides, previous to and following the fieldwork (at least), as observed by the fieldwork team when arriving at and leaving the barrier island. Between February 8th and 12th the tidal level was above 1.5 m MSL on 8 occasions, however overwash may have occurred more times (on 15 occasions the tidal level was above 1.2 m MSL). One overwash event (one tidal cycle) caused an accretion of +3.4 m^3/m, during complete overwash conditions; therefore

it is possible that the overall sediment accumulation during the spring tide period was between 20 and 30 m^3/m.

In the case of GO.3, the washover mouth had an elevation of 3.28 m MSL and the fan accreted +4.7 m^3/m and the mouth was lowered 14 cm. Since most of the accretion was noticed on the distal fan, it must have been deposited during the complete overwash stage. The complete overwash started when the tide level was close to 1.5 m (Figure 4.8b). Similarly to GO.1, the occurrence of overwash events did not start or end during the period of the GO.3 fieldwork campaign. Between February 17th and 21st, the tidal level was above 1.5 m on 5 occasions. Assuming that during most of these tides complete overwash occurred, then it can be hypothesised that more than +20 m^3/m were deposited on the washover lobe.

During the winters of 2000/2001, 2001/2002, and 2002/2003, tidal levels above 1.2 m and 1.5 m occurred on average 134 high tides/year (18% of total tides) and 33 high tides/year (4.5% of total tides), respectively. The average number of days with non-storm SW-W waves higher than 1 m was 78 days/year (21% of total days; derived from the data presented in Costa *el al.*, 2001). Therefore, the conditions recorded during the fieldwork campaigns GO.1 and GO.3 have a probability of occurrence of about 1% to 4% (i.e. less than 10 high-tides/year for complete overwash and about 30 high-tides/year for overwash). Assuming that from the 10 spring high tides that occur during the winter each year, 5 encounter the appropriate foreshore morphology, then about 100 m^3/m/year can be potentially deposited on the crest or fan. Therefore, non-storm overwash processes may have an important role in the sedimentary evolution of this barrier. The SW-W storm waves (H_s > 3 m) that can lead to storm overwash generally occur less than 1% of the year (Costa *et al.*, 2001), and may induce more rapid but less frequent sedimentary changes on Barreta Island. Moreover, minor storms, with wave heights close to 3 m, which occur during neap tides, may not induce storm overwash.

Storm-induced overwash situations have frequently been described in the literature. The wave height that promotes overwash and the volume of sediments deposited by overwash can vary significantly (Table 2.1, section 2.3). The studies relate storm-induced overwash changes with wave heights that varied from less than 4 m [e.g. Storm northeaster of March 1975 (Leatherman, 1976)] to more than 9 m [e.g. Halloween Eve Storm of 1991 (FitzGerald *et al.*, 1994) and Hurricane George of 1998 (Stone *et al.*, 2004)]. Depositional volumes varied between less than 5 m^3/m [e.g. Assateague Island, March 1973 Northeastern (Fisher *et al.*, 1974) and Devereaux Beach, Halloween Eve Storm of 1991 (FitzGerald *et al.*, 1994)] up to more than 50 m^3/m [e.g. Trabucador Bar, October 1990 Storm (Guillén *et al.*, 1994; Sànchez-Arcilla and Jiménez, 1994) and Santa Rosa Island, Hurricane Opal of 1995 (Stone *et al.*, 2004)].

The volumes recorded during the GO.1 and GO.3 fieldwork campaigns, extrapolated to the entire spring tide period were similar to the volumes recorded for some storm conditions (Table 2.1, section 2.3). However, unlike the storms, the non-storm spring tide overwash can be repeated up to about 30 times during each winter. Some of the overwash volumes found in the literature (e.g. Deveraux Beach, Table 2.1, section 2.3) were similar to the GO.3 washover lobe during a single tidal cycle, but the waves were much higher (9.1 m, FitzGerald *et al.*, 1994). The main difference was that the adjacent beach of the fieldwork washovers was in dynamic equilibrium or in accretion on the upper part, however, the storms that induce overwash are more frequently accompanied by beach erosion [e.g., Nauset Spit, February 1978 Storm (Leatherman and Zaremba, 1987)], and infrequently beach accretion [Assateague Island, October 1973 Tropical Storm Gilda (Leatherman, 1976)].

The comparison between storm overwash deposition and non-storm deposition showed that the volume variations can be similar, but the situations in which both occur are different. The non-storm overwash are only possible if the barrier has a low-elevation crest but storm

overwash can occur hypothetically on all barriers given sufficient sea level super-elevation. The storm intensity is therefore a very important factor in determining the location and the importance of overwash in the evolution of a barrier. However, the spring high tides on certain coasts can be of the outmost importance in inducing overwash under non-storm conditions or providing the necessary super-elevation to increase the magnitude of storm overwash. Further, it is possible that during storms washover crest is eroded, and consequently non-storm overwash conditions are achieved during the next spring tides. In the study area, overwash processes were observed in subsequent winters after fieldwork was done (2004 and 2005). This implies that the crest was subsequently eroded, most likely during storms, in order to allow the maintenance of the overwash threshold conditions. The combination of storms and non-storm overwash may be very effective for inland sediment transport, since non-storm overwash induces accretion of the crest and storms may promote crest erosion that allows landward displacement of sediments. Therefore, these two situations can act to complement each other, increasing the magnitude of the overwash sediment transport in the barriers evolution.

In the case of the washover lobes, the erosion of the mouth was noticed even during non-storm conditions, and it is likely that the same happens during storms. This reinforcement of processes at the washover mouth may justify the relatively rapid enlargement of the mouth and consequent coalescence of consecutive lobes. In fact, the washover lobe of GO.1 (2001) coalesced with the washover plain before GO.2 (2002), and the washover lobe of GO.2 coalesced with the washover plain before GO.3 (2003).

4.5. CONCLUSIONS

A comprehensive set of data was acquired for non-storm overwash occurring on a low barrier island. Three fieldwork campaigns were performed: GO.1 (winter of 2001), GO.2 (winter of 2002), and GO.3 (winter of 2003), on western Barreta Island. Overwash events were measured during GO.1 and GO.3 fieldwork campaigns. The overwash dynamics were distinct for two separated washover morphologies: washover plains and washover lobes. The washover plains were featureless gently landward dipping surfaces, and the overwash event started when the seawater overtopped the crest of the washover. The washover lobes had a distinct teardrop shape in plan-view, and the overwash flow was firstly constrained in the washover mouth and channel and ultimately spread on the washover fan.

The same magnitude of waves ($H_s \approx 1$ m), and similar spring high tides (tidal level ≈ 1.7 m), were recorded for both campaigns. During both GO.1 and GO.3 complete overwash at the high tide slack was recorded. However, morphological changes, mixing depths and transport pattern were different for the washover plains of GO.1 and GO.3, and the washover lobe of GO.3.

The washover plains underwent accretion as a wedge shape thin layer, thicker over the crest and negligible on the landward parts of the terrace. This washover deposit configuration is related with the decrease in flow capacity as it progresses through the washover terrace, and also with the landward decrease of the frequency of overwash intrusions. Accordingly, the mixing depth distribution over the washover plain showed that the washover crest was the most dynamic part, and that shallow mixing depths were observed in the interior parts, subjected to low frequency and low depth overwash flows. The tracer transport patterns showed that during the early stages of overwash, the upper beach face was subjected to both onshore sediment transport to the washover crest and longshore transport due to an oblique

component of the wave run-up. As overwash frequency increased the onshore sediment transport became more significant, dominantly shore-normal. The sediment movement inside the washover plain during an overwash event can be divided into three main stages: Stage 1 - Crest Accretion, Stage 2 - Onshore Flow, and Stage 3 - Dynamic Equilibrium. Stage 1 is characterised by the early overwash flows, where the crest was overtopped but the progression of the flow was inhibited by the friction and infiltration on a gentle landward angle crest. The Stage 2 corresponds to a higher tidal level that induces an increase in overwash frequency and intrusion, and the occurrence of complete overwash. The overwash flow was faster and had the capacity to transport sand for variable distances according to the overwash intrusion. Once the tide started to drop Stage 3 begins, inducing almost negligible morphological changes even though overwash continues to occur. This asymmetrical behaviour was probably due to the adjustment of the sedimentary environment to the higher magnitude overwash at the high tide slack (Stage 2).

The washover lobe underwent erosion of the mouth and channel, and accretion on the washover fan. Determination of the mixing depth showed that the most dynamic parts were the washover mouth and distal fan. The sediment transport patterns obtained with the tracers showed the landward progression of the sediments entering the washover mouth. Unlike the washover plain, the sediment transport inside the washover lobe can be characterised by one onshore flow stage, but with variations in magnitude. In places where the run up flow running on the top of the beach face encountered the washover mouth, the wave up-rush was converted into overwash flow as it overtopped the washover mouth. The dune erosion due to wave-generated run up impingement caused the deepening and enlargement of the washover mouth. Once the mouth was overwashed, the lateral restriction of the flow in the channel together with the steeper landward slope induced the increase of the flow velocity and the subsequent erosion. The bottom friction and infiltration on the fan surface, together with a

lateral spreading possible due to the absence of dunes on the lagoon side of the barrier induced a deceleration of the flow and the consequent sand deposition. With the drop of the tide, the overwash intrusion was reduced and the flow stopped in the channel thus causing the deposition of the sand.

The overwash measured during fieldwork correspond to non-storm overwash events. The main factors governing the occurrence of non-storm overwash on the study area were the joint occurrence of: (i) typical winter waves, (ii) equinoctial spring high tides, (iii) absence of well-developed beach berms, and (iv) washover crest/mouth below the dynamic threshold of Z_{crest} < high tide + 2.1 m.

Non-storm overwash will occur repeatedly provided that the limiting factors are satisfied. If the average accretion measured for a single overwash event is considered to be representative of the entire spring tide period, an estimate of more than +20 m^3/m could have occurred for both fieldwork periods. This deposition has the same magnitude as the storm overwash deposition found in the literature (33 ± 42 m^3/m), for wave heights of 6.6 ± 2.2 m. The non-storm overwash oceanographic factors have a probability of occurrence of about 1% to 4% for the study area, while storm waves occur less than 1% of the year (Costa *et al.*, 2001). The re-occurrence of non-storm overwash for half of the situations when threshold conditions (waves and tides) are achieved could lead to the deposition of about 100 m^3/m/year.

In the study area, both storm- and non-storm-overwash occur. The occurrence of storms may be essential for the maintenance of the morphological factors limiting non-storm overwash (Z_{Crest} < high tide + 2.1 m and absence of beach berm). The storms and non-storm overwash are probably complementary for inland sediment transport, since non-storm overwash develops the crest that seems to be eroded during storms. In the case of the washover lobes, the erosion of the mouth was noticed during non-storm conditions, and is

probable during storms. The typical succession of events can be therefore described in the following steps: (1) generation of washover lobes by storm-overwash; (2) erosion of the mouth and deposition on the fan during storms and non-storm overwash; (3) enlargement of the mouth and coalescence of washover lobes during storms and non-storm overwash; (4) development of a washover plain by storms or non-storm overwash; (5a) accretion of the washover crest during non-storm overwash, or (5b) erosion of the washover crest during storms; (6a) end of overwash processes or (6b) continuation of overwash processes (steps 5a and 5b).